

Effect of Axle and Dual Spacing on Horizontal Strain Distribution for Flexible Pavement

Dr. Abdul Haq H. Abed Ali
Dept. Of HWY'S & Transportation
College Of Engineering
University Of Al – Mustansiriya
Lecture

Mrs. Maha O. Al-Mumais Dept.
Of HWY'S & Transportation
College Of Engineering
University Of Al – Mustansiriya
Lecture

Abstract

The flexible pavement layers attach each day by thousands of several types of vehicles according to axle spacing and distribution between each tires (dual spacing) at same axle. These different types of wheel and tires generate deformations or horizontal strain caused fatigue of pavement then reduced pavement life.

In this work using three layers system with linear visco-elastic hot mixture layer. Visco-elastic properties obtained from creep test under static load. Kenlayer program used to determine horizontal strain under applied load. It's concluded that when the axle spacing and dual spacing increase the horizontal strain over lapping reduced. The study obvious that when axle spacing increases from 273 cm (sonata car) till 1524 cm (truck 3-S2) the horizontal strain decreases about 30% .

Key Words: Axle Spacing, Dual Spacing, Visco-elastic, horizontal strain, Flexible Pavement.

الخلاصة

تتعرض الخرسانة الاسفلتية كل يوم الى الالاف من الاحمال المرورية المختلفة من حيث المسافة بين المحاور و كذلك المسافة بين الاطارات لنفس المحور. هذه الانواع المختلفة من المحاور و الاطارات تولد تشوهات او هبوط في طبقات التبليط الاسفلتي و حدوث تداخل في هذه التشوهات مما سبب فشل التبليط و تقليل العمر الخدمي له. في هذا البحث و لغرض دراسة توزيع هذه التشوهات بالطبقات تم بناء نموذج يتكون من ثلاثة طبقات و على فرض بان طبقة التبليط الاسفلتي تتصرف كمادة لزجة-مرنة حيث تم استخدام النتائج التي تم الحصول عليها من فحص الزحف لنماذج الخرسانة الاسفلتية المصممة بطريقة مارشال.

استخدم برنامج Kenlayer لحساب قيمة الهبوط اسفل الحمل المسلط، حيث لوحظ من خلال البحث بانها كلما تزداد المسافة بين المحاور يقل تأثير منطقة تداخل المحاور المسببة للهبوط كما لوحظ نفس التأثير عند زيادة المسافة بين الاطارات. بينت الدراسة ان المنطقة المتأثرة بتداخل تأثير المحاور قد انخفضت بمقدار 30% بالنسبة لسيارة سوناتا (273 سم) مقارنة بسيارة الحمل 3-S2 (1524 سم).

1- Introduction

Hot mixture asphalt (HMA) is a composite material of aggregates with asphalt cement as a binder. The performance of HMA is governed by the properties of aggregate, properties of asphalt cement, the usage of asphalt cement modifiers, and the asphalt aggregate interactions. The HMA shows discrete behavior as relative positions of aggregate particles change during deformation. The performance of HMA is also sensitive to the traffic loading rate, moisture damages, and environmental temperature Gedafa ⁽¹⁾ and Chen ⁽²⁾.

There are several alternatives of conventional flexible pavement sections were varied in the thickness of the surface, base and subbase course, type of axle load, contact pressure, radius of contact area,..... etc. Conventional flexible pavements are three layered system of surface, base and subgrade layer as shown in Figure (1).

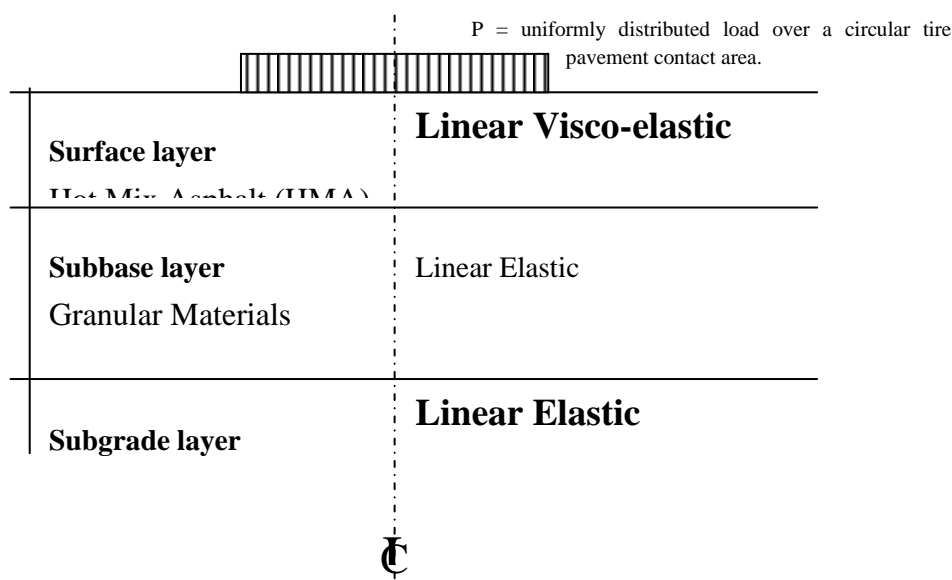


Figure (1): Employing Three Layer Systems.

2- The Applied Load

Axle load was used according to the type of vehicle. Tire constant area is assumed circle shape with actual radius. The levels of tire pressure were used for the selected axle and for the truck the tire pressure assume 95 psi according to SCRB Specification ⁽³⁾.

The vehicle speed relates to the time duration of loading (the duration time increased when the vehicle speed is decreased or decreased with increased vehicle speed). Two duration times are used to simulate the moving load 0.1 sec for 40 mph (64Km/h) and 0.05 sec for 60 mph (96 Km/h) Huang ⁽⁴⁾.

3- Environmental Factors

The performance of the flexible pavement depends on the several environmental factors. The variation in the temperature of the asphalt layer is included in the proposed method because the changes in temperature affect on the visco-elastic properties of the bituminous layer. Two periods per year are used to simulate effect of weather factors, as shown in table (1).

Table (1): Characteristics of Each Period through One Year.

One Year	Periods	MMAT [*] , °C
	First Period, Months (Oct. Mar.)	25
	Second Period, Months (Apr. Sep.)	40

** MMAT : Mean Monthly Air Temperature °C by Ahmed, N., G. ⁽⁵⁾*

The temperature of the HMA layer can be predicted based on the following equation, which used in the Asphalt Institute ⁽⁶⁾ and depending on the air temperature;

$$T_{HMA} = T_{air} \left[1 + \frac{76.2}{Z + 304.8} \right] - \frac{84.7}{Z + 304.8} + 3.3 \dots\dots\dots (1)$$

Where:-

T_{HMA} : the temperature of the HMA layer (°C).

T_{air} : mean Monthly Air Temperature MMAT (°C).

Z : the depth under the surface (mm).

This equation is used to estimate temperature of the HMA layer at the (20-mm) under the surface and changed with the depth or thickness of layer.

4- Material properties

The geometry of the selected pavement structure was consisted of three layers system. These layers are: -

- 1- Surface layer consists of asphaltic materials (HMA).
- 2- Subbase layer consists of granular materials
- 3- Subgrade layer or soil layer.

In general the following data, the thickness of each layer except the subgrade layer which is assumed infinite thickness, the visco-elastic properties for surface layer, and elastic properties for another layer and Poisson’s ratio for all layers. The methods that used to obtain these parameters are described in the following sections.

4-1 Properties of Hot Mixture Asphalt Layer

Heukelom and Klomp ⁽⁷⁾ calculate the stiffness of the asphalt mixture (E_m) from the stiffness of the asphalt binder using the following equation;

$$E_m = E_{asp} \left[1 + \left(\frac{2.5}{n} \right) \left(\frac{C_v}{1 - C_v} \right) \right]^n \dots\dots\dots(2)$$

Where:-

$$n = 0.83 \log_{10} \left(\frac{4 * 10^5}{E_{asp}} \right) \dots\dots\dots(3)$$

$$C_v = \frac{Volume\ of\ aggregate}{V_{aggregate} + V_{asphalt}} \dots\dots\dots(4)$$

E_m = Stiffness of asphalt mixture

C_v = Coefficient of concentration

E_{asp} = Stiffness of asphalt binder (kg/cm^2)

The stiffness of asphalt binder was calculated using the Van der Poel nomograph (1954) Yoder ⁽⁸⁾. The value of Poisson’s ratio for HMA layer is 0.4. The thickness of asphaltic layer is assumed to be 4 in (10 cm) SCRB Specification ⁽³⁾. The parameter for this model can be calculated by assuming generalized model shown in figure (2).

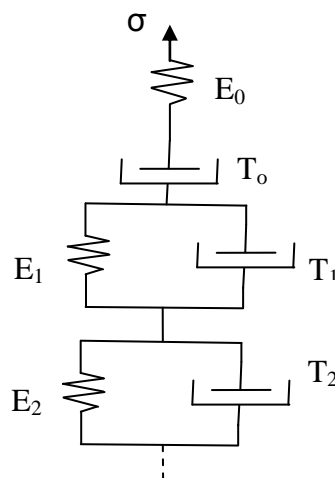


Figure (2): Generalized Model for Visco-elastic Materials

Huang ⁽⁴⁾ explained that a single Kelvin model is usually not sufficient to cover the long period of time which the retarded strain takes place and a number of Kelvin models may be needed. Therefore, the generalized model is used to determine the visco-elastic constants E_o , T_o , E_t and T_t contain of one Maxwell model and two Kelvin models connected in series as shown in Figure (2). The parameters E_o , T_o , E_t and T_t shown in generalized model can be calculated from strain time curve for the results obtained from creep test under static load as shown in table 2.

Table (2): Creep results with time (Al-Haddad, 2005)⁽⁹⁾

<i>Time (sec)</i>	<i>Creep Compliance</i>
0	0.0001826
6	0.0003654
15	0.0007303
30	0.0010555
60	0.0015022
120	0.0019894
240	0.0029029
480	0.0036133
900	0.0044253
1800	0.0056026

4-2 Properties of Subbase Layer

The elastic modulus of the granular subbase layer was considered constant in the proposed constructed model. It was to be (18×10^3 Psi) corresponding SCRB specification ⁽³⁾ for class C and D. The Poisson's ratio for the granular material depends on the degree of compaction ranges from 0.3 to 0.5 as shown by Bowles ⁽¹⁰⁾. The typical value was taken it ($\mu=0.45$). The thickness of the subbase layer was taken equal to 8 in (20.3 cm) for the selected structure.

4-3 Properties of Subgrade Layer

The elastic modulus of the subgrade layer could be estimated from CBR test. In the proposed model, the magnitude of the modulus of subgrade was assumed to be constant with CBR (value > 4) and equal to (6×10^3 Psi). Poisson's ratio for subgrade soil, depending on the degree of soil cohesion, changes from 0.3 to 0.5 as shown by Bowles ⁽¹⁰⁾ and Fanous, Coree and Wood ⁽¹²⁾. The typical value was taken to be 0.45.

5- Geometric of Axle and Dual Spacing

In this study, Kenlayer computer program is used to calculate the deformation under wheel loads and the reason of using such program that the deformation can calculate at the surface of the pavement, at depth 10.16 cm (below the first layer), and at depth 30.48 cm (below the second layer). Figure (3) shows dividing contact area below the tire of sonata (2010).

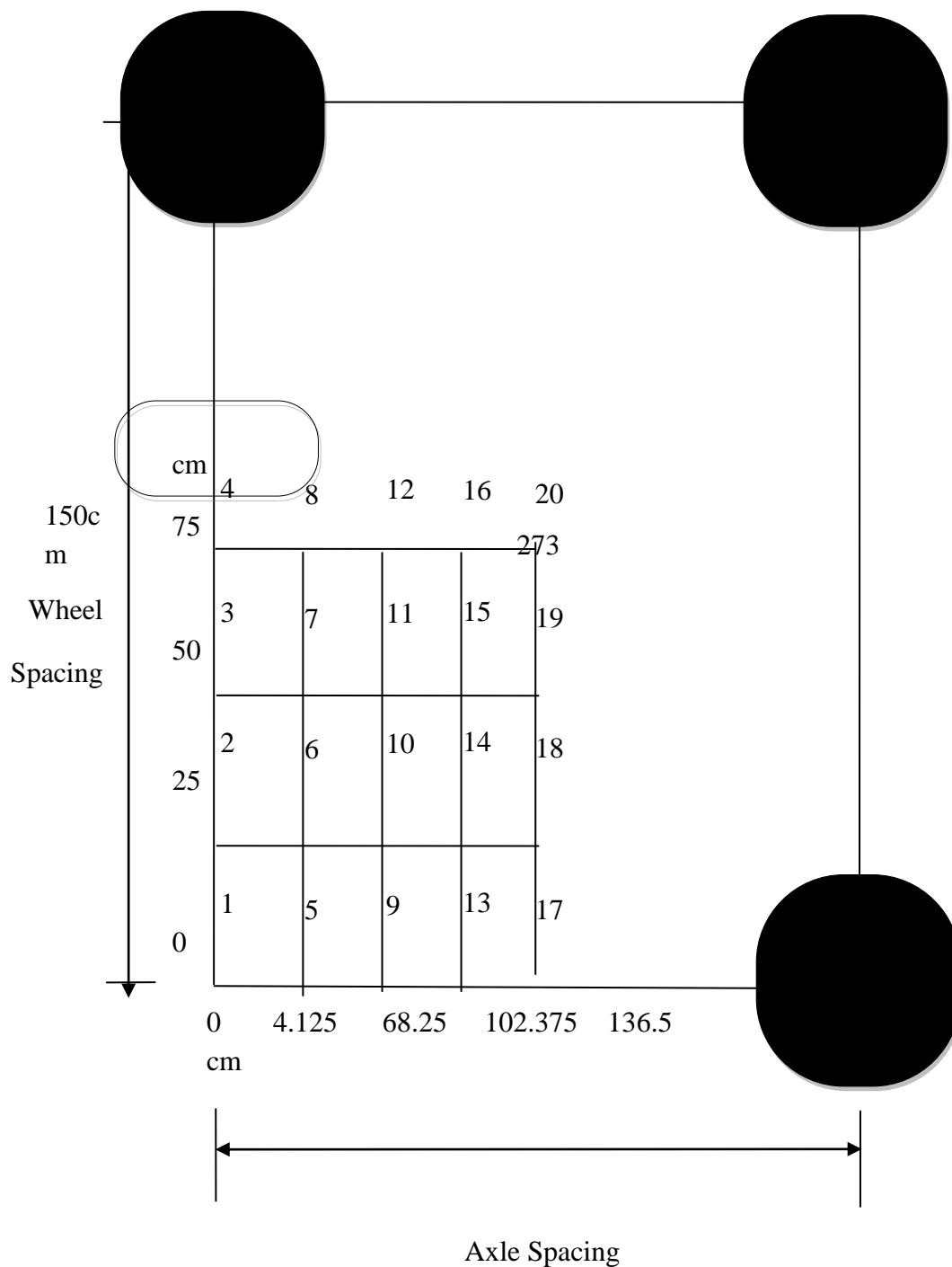


Figure (3): Plan view for axle of sonata 2010

Figure (4) shows dividing contact area below the tire of truck 3-S2.

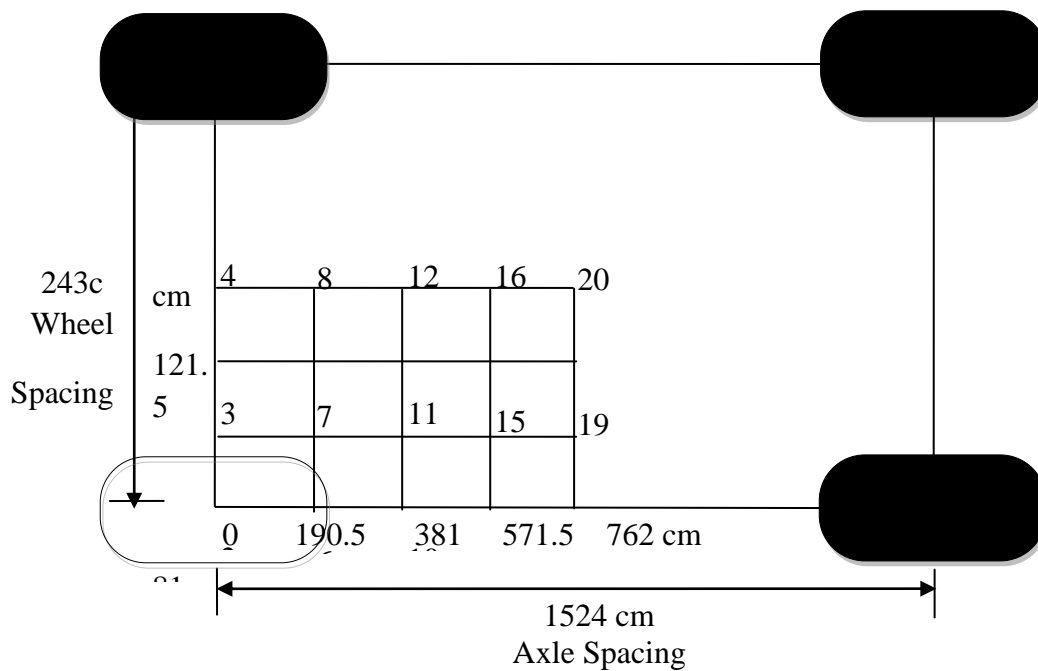


Figure (4): Plan view for axle of truck 3-S2.

Figure (5); shows the deformation (horizontal strain at the surface of the pavement) occur due to (sonata 2010)

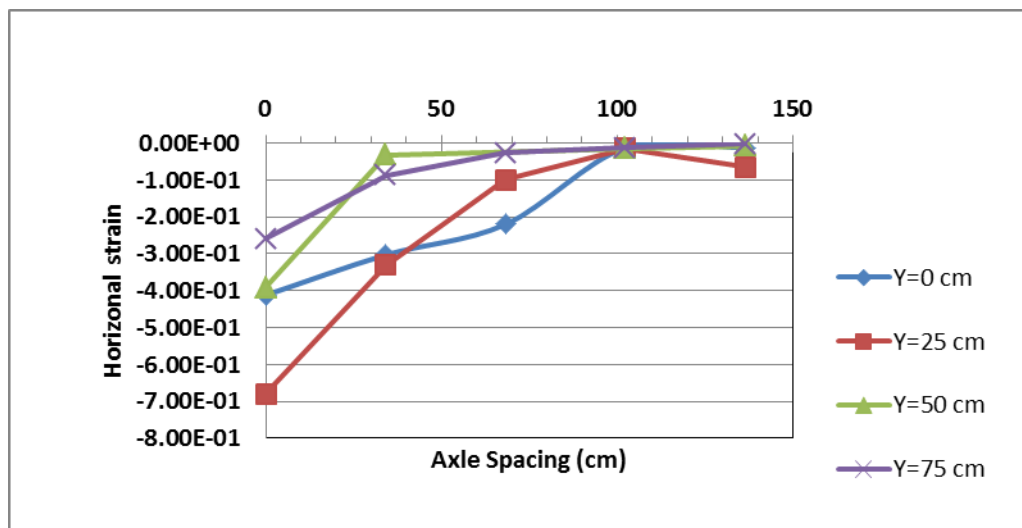


Figure 5: The relationship between the surface horizontal strain and spacing of axle

Figure (6); shows the deformation (horizontal strain below the first layer of the pavement) occur due to (sonata 2010)

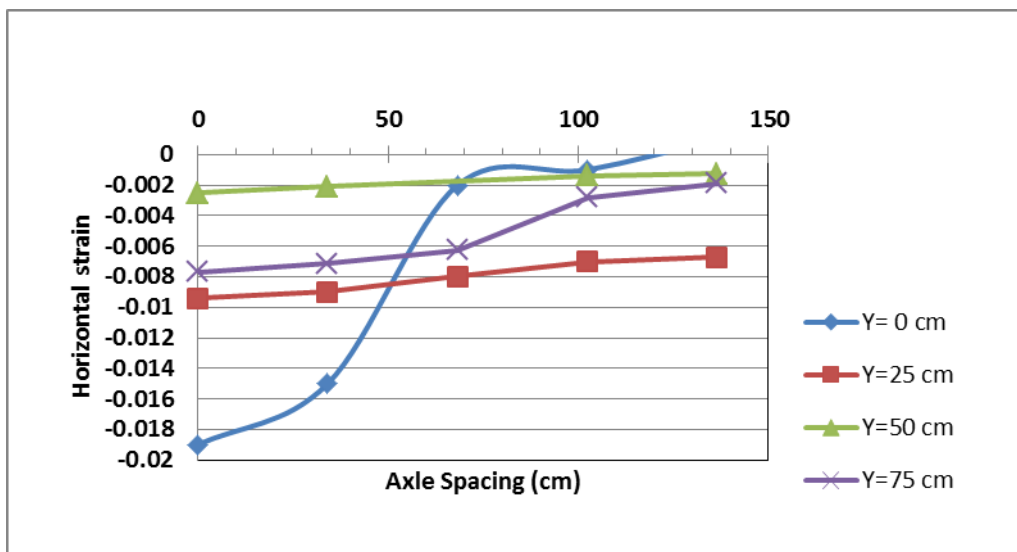


Figure 6: The relationship between the horizontal strain at 1st interface and spacing of axle

Figure (7); shows the deformation (horizontal strain below the second layer of the pavement) occur due to (sonata 2010)

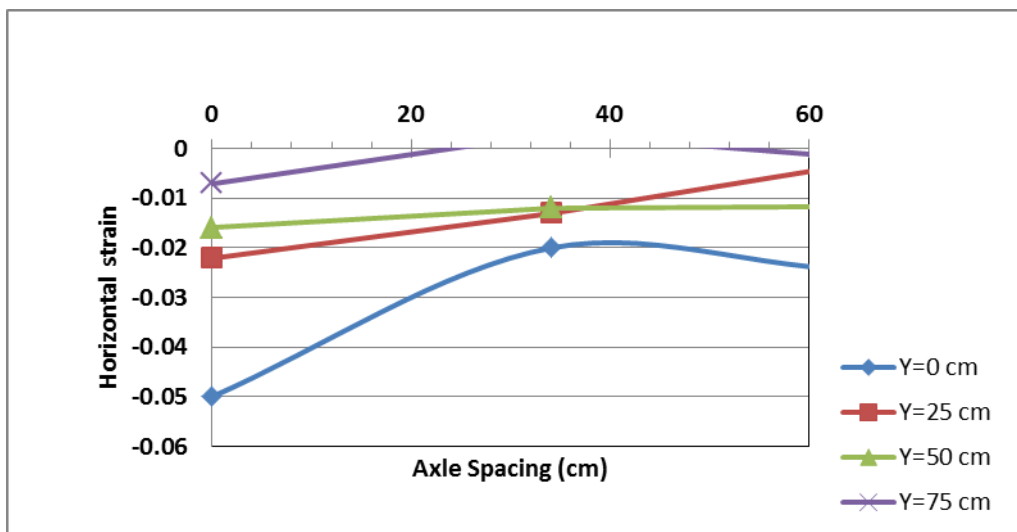


Figure 7: The relationship between the horizontal strain at 2nd interface and spacing of axle

Figure (8); shows the deformation (horizontal strain at the surface of the pavement) occur due to (Nissan Qashqai)

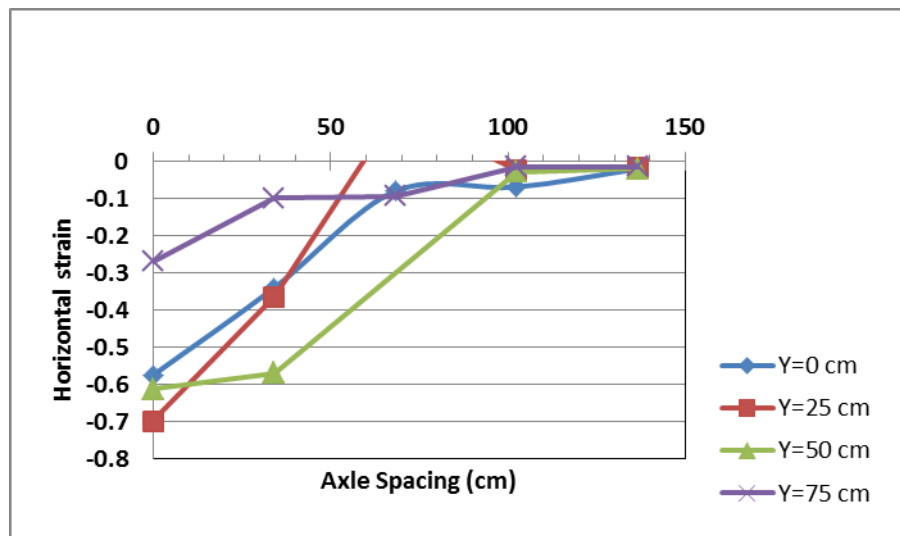


Figure 8: The relationship between the surface horizontal strain and spacing of axle

Figure (9) shows the deformation (horizontal strain below the first layer of the pavement) occur due to (Nissan Qashqai)

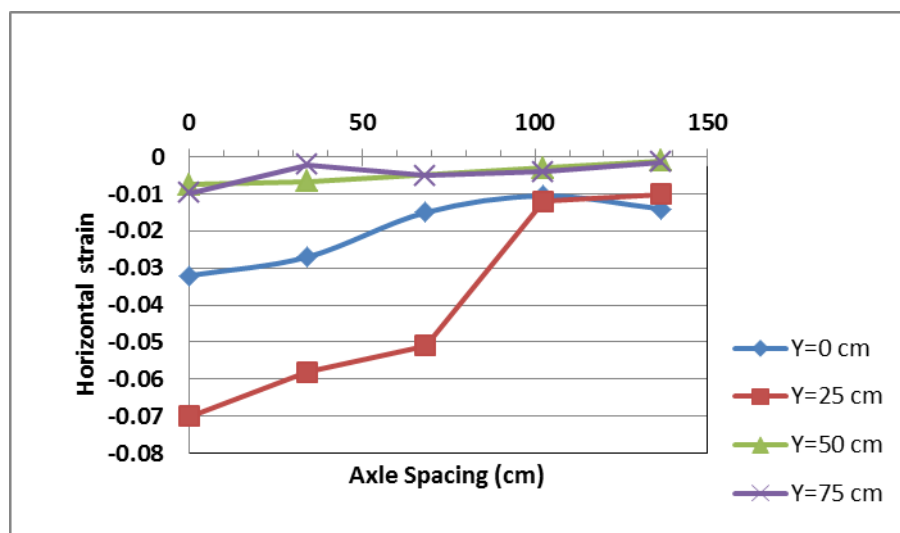


Figure 9: The relationship between horizontal strain at 1st interface and spacing of axle

Figure 10 shows the deformation (horizontal strain below the second layer of the pavement) occur due to (Nissan Qashqai)

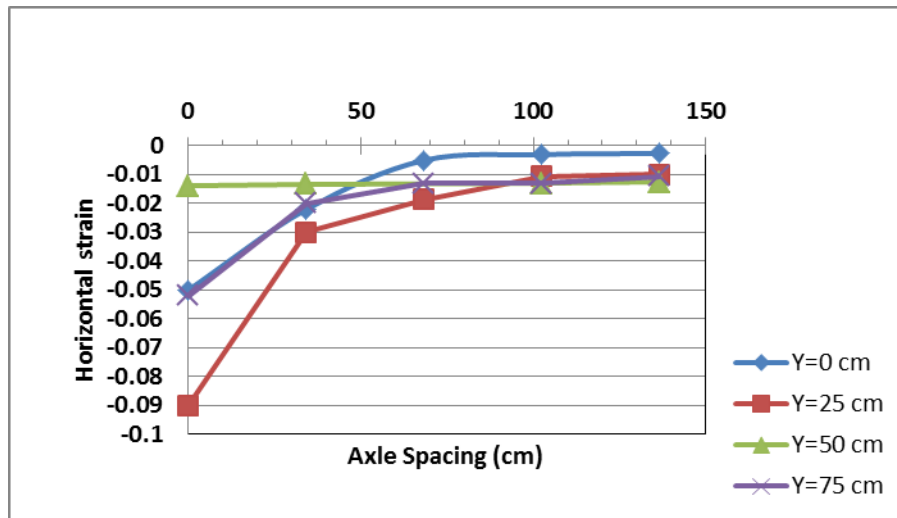


Figure 10: The relationship between the Horizontal strain at 2nd interface and spacing of axle

Figure 11 shows the deformation (horizontal strain at the surface of the pavement) occur due to Truck 2-S2

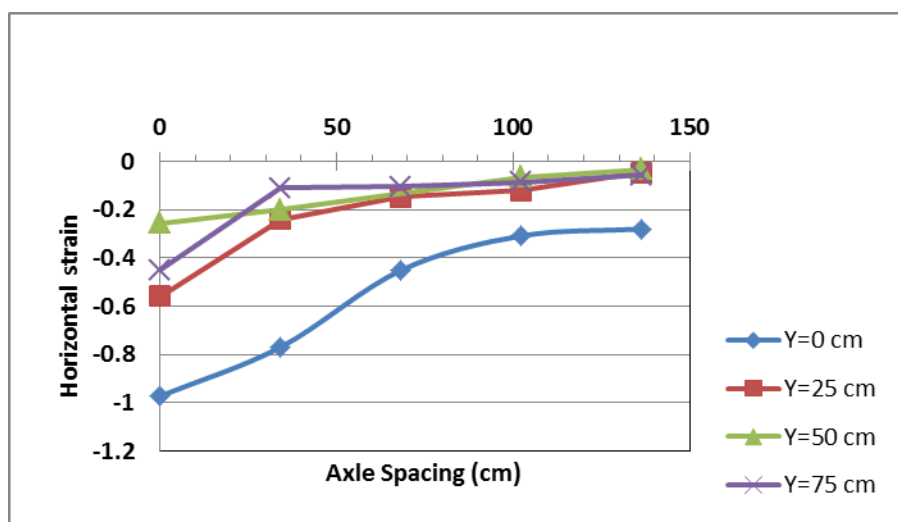


Figure 11: The relationship between the surface horizontal strain and spacing of axle

Figure 12 shows the deformation (horizontal strain below the first layer of the pavement) occur due to Truck 2-S2

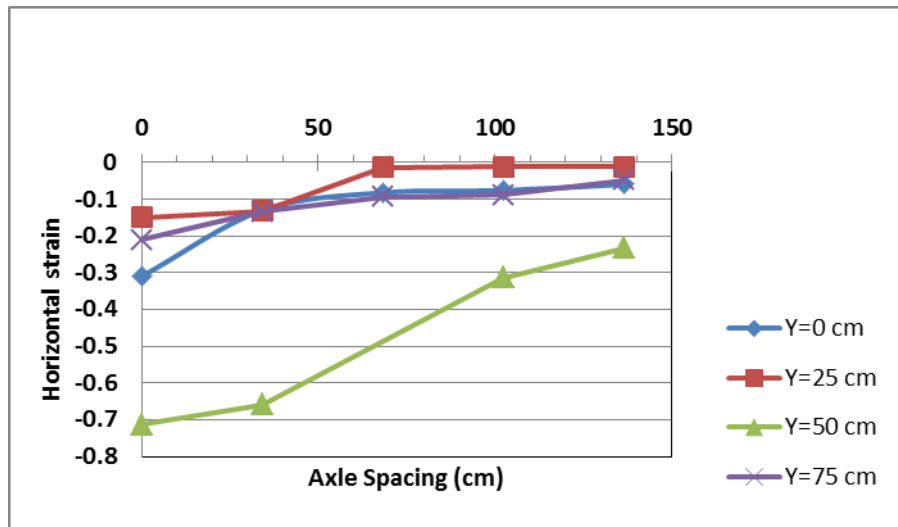


Figure 12: The relationship between the horizontal strain at 1st interface and spacing of axle

Figure 13 shows the deformation (horizontal strain below the second layer of the pavement) occur due to Truck 2-S2

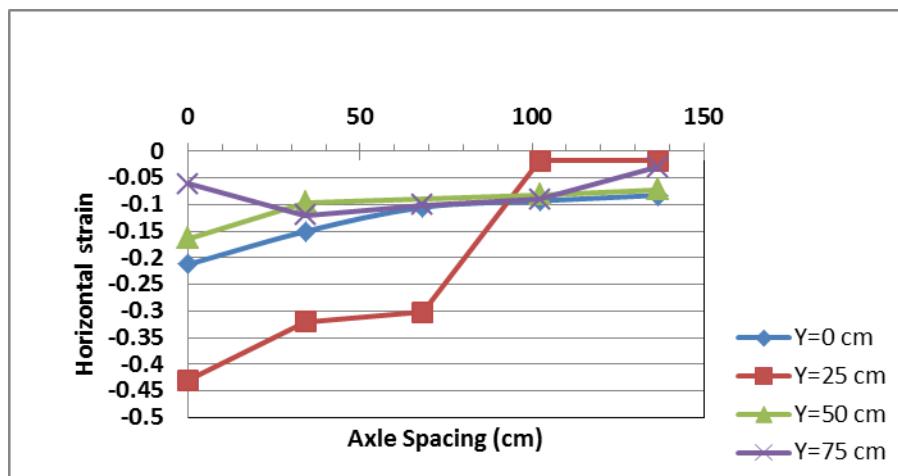


Figure 13: The relationship between the horizontal strain at 2nd interface and spacing of axle

Figure 14 shows the deformations (horizontal strain at the surface of the pavement) occur due to Truck 3-S2.

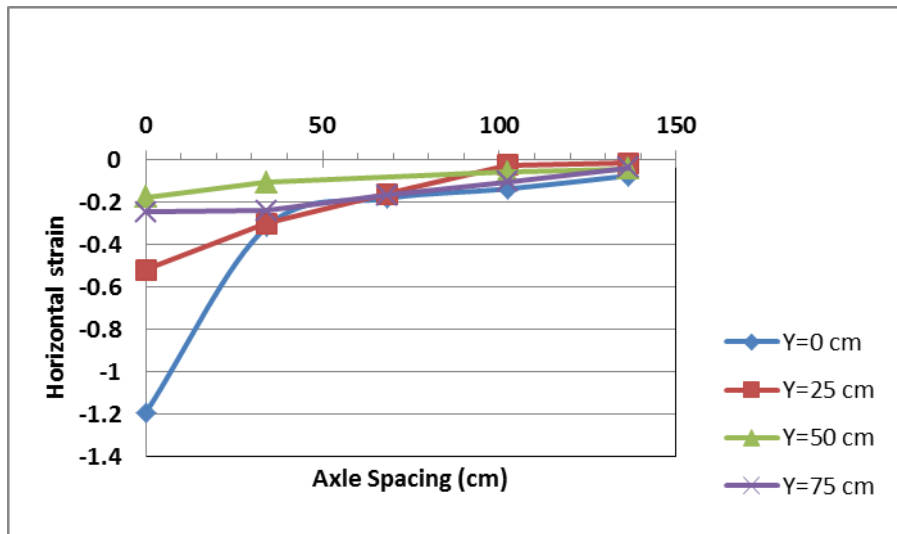


Figure 14: The relationship between the surface horizontal strain and spacing of axle

Figure 15 shows the deformations (horizontal strain below the first layer of the pavement) occur due to Truck 3-S2

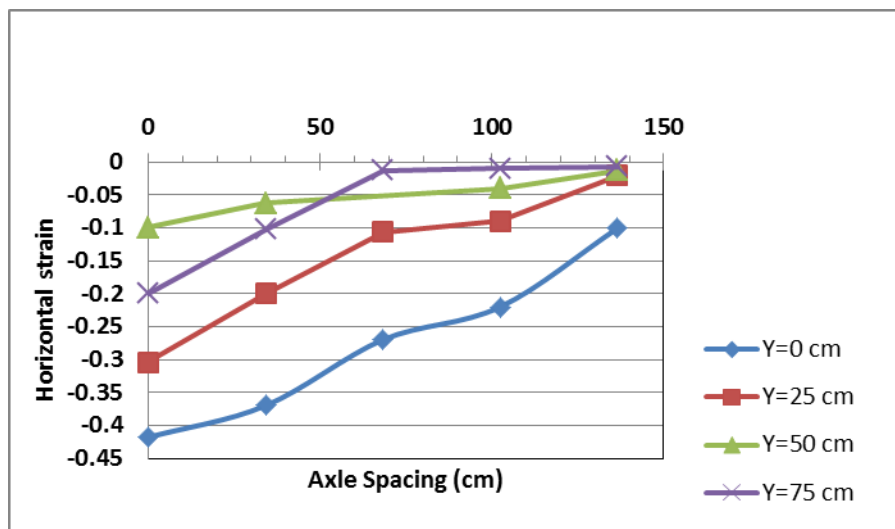


Figure 15: The relationship between the horizontal strain at 1st interface and spacing of axle

Figure 16 shows the deformations (horizontal strain below the second layer of the pavement) occur due to Truck 3-S2

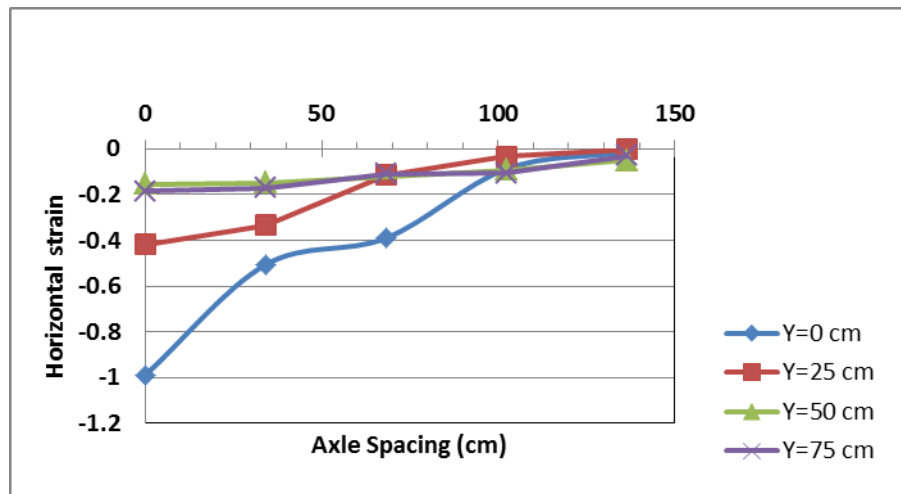
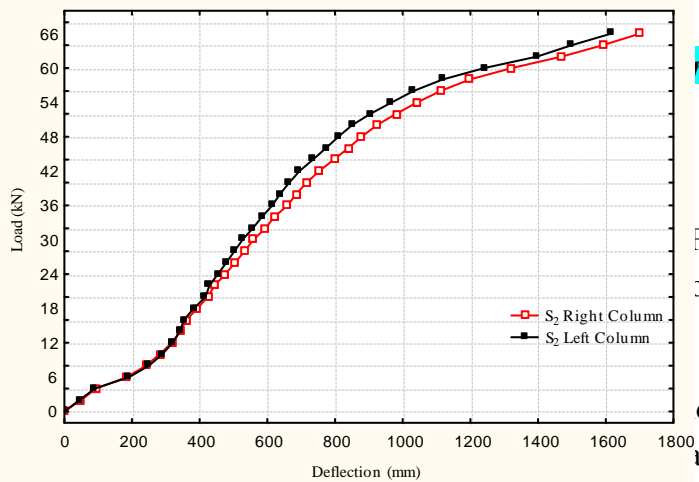


Figure 16: The relationship between the horizontal strain at 2nd interface and spacing of axle

6- Conclusion:

The following conclusions are obtained from the theoretical and experimental works.

1. The horizontal strain in pavement has more influence on layer properties & the assumptions of visco-elastic properties for surface layer are more realistic.
2. When axle spacing increased the generate horizontal strain reduced & so decrease over lapping stresses between axle and another.
3. When dual spacing increased the horizontal strain decreased.



Flexible Pavement Performance Using Kenlayer and
of civil engineering, Kansas State University,

ou, "Development of 3-D Finite Element Model for
il of the Chinese institute of engineering, vol. 27, No.

5, pp. 707-717.

3. State Cooperation of Roads and Bridge (SCRB), Section R9 (2003): "Hot Mix Asphalt Concrete Pavement", Iraq Standard Specification, Ministry of Housing and Construction, Department of Design and Study.
4. Huang, Y.H., "Pavement Analysis and Design", Prentice Hall, New Jersey, 1993.
5. Ahmed, N., G., "The Development of Models for the Prediction of Thermal Cracking in Flexible Pavements" Ph.D. Thesis, College of Engineering, University of Baghdad-2002.
6. Asphalt Institute, "Mix Design Methods for Asphalt Concrete", Manual Series No.2 (MS-2), May 1984.
7. Heukelom, W. and Klomp, A.J.G., "Dynamic Testing as a Means of Controlling Pavements During and after construction", 1st International Conference on the Structure Design of Asphalt Pavements, 1964, pp 667-685.
8. Yoder, E. J., and Witczak, M. W., "Principles of Pavement Design", 2nd. Addition, John Wiley and Sons, 1975.
9. Al-Haddad, A., H., "Development of Model for Fatigue Prediction in Flexible Pavement" Ph.D. Thesis, College of Engineering, University of Al-Mustansiriyah-2005.
10. Bowles J., E., "Foundation Analysis and Design", 3rd edition, McGraw-Hill Book Company, 1982.
11. AASHTO, "AASHTO Guide for Design of Pavement Structures", 1986.
12. Fouad Fanous, Brian Coree, and Doug Wood "Response of IOWA Pavements to a Tracked Agricultural Vehicle" 2000. Sponsored by the highway division of the IOWA Department of Transportation Iowa Dot project HR-1075, CTRE Management project 99-51.